

TR 66095

MARCH

1966

UNLIMITED

ROYAL AIRCRAFT ESTABLISHMENT

TECHNICAL REPORT No. 66095

AD 638210



**THE MOBILITY OF THE
SURFACE ATOMS OF
COPPER AND SILVER
EVAPORATED DEPOSITS**

by

Rosalie Brandon

F. J. Bradshaw

CLEARINGHOUSE FOR FEDERAL SCIENTIFIC AND TECHNICAL INFORMATION		
Hardcopy	Microfiche	
\$ 2.00	\$ 0.50	38 pp
ARCHIVE COPY		

Code 1

SEP 14 1966
D.

MINISTRY OF AVIATION
FARNBOROUGH HANTS

ROYAL AIRCRAFT ESTABLISHMENT

Technical Report No. 66095

March 1966

THE MOBILITY OF THE SURFACE ATOMS OF COPPER AND SILVER EVAPORATED DEPOSITS

by

Rosalie Brandon

F. J. Bradshaw

SUMMARY

Estimates of the surface self-diffusion coefficients of evaporated deposits were made from (1) the spread of material into a shadow cast by the placing of an object between source and substrate, (2) the decay on annealing of the step produced in a metal film deposited onto a mica surface with a cleavage step, (3) the thermal grooving of grain boundaries in deposited films, and (4) the growth of holes in thin films. Rate laws were proposed and verified experimentally for step smoothing and the growth of holes.

Departmental Reference: CPM 67

		<u>Page</u>
1	INTRODUCTION	5
2	THEORY	6
	2.1 The decay of a step, (Method 2)	6
	2.2 Smoothing of a step whose height is increasing at a constant rate, (Method 1)	7
	2.3 Grain boundary grooving, (Method 3)	8
	2.4 The growth of holes in thin evaporated films, (Method 4)	8
	2.5 The surface energy, γ_s	10
3	EXPERIMENTAL	11
4	THE SMOOTHING OF A STEP WHOSE HEIGHT IS INCREASING AT A CONSTANT RATE, (Method 1)	12
	4.1 Introduction	12
	4.2 Experimental	12
	4.3 Results	13
	4.4 Discussion	13
5	THE DECAY OF A STEP, (Method 2)	14
	5.1 Introduction	14
	5.2 Experimental	14
	5.2.1 Vacuum anneals	14
	5.2.2 Air anneals	15
	5.3 Results	15
	5.4 Discussion	16
6	GRAIN BOUNDARY GROOVING, (Method 3)	17
	6.1 Introduction	17
	6.2 Experimental	17
	6.3 Results	17
	6.4 Discussion	18
7	THE GROWTH OF HOLES IN THIN EVAPORATED FILMS (Method 4)	18
	7.1 Introduction	18
	7.2 Experimental	19
	7.3 Results	19
	7.4 Discussion	21
8	CONCLUSIONS	21
	Symbols	22
	References	23
	Illustrations	Figures 1-20
	Detachable abstract cards	-

ILLUSTRATIONS

	<u>Fig.</u>
The smoothing of a step of height α , due to surface diffusion	1
The shape of a grain boundary groove due to surface diffusion	2
The profile of a hole in an evaporated film which is growing by surface diffusion	3
Profile of hole edge	4
The variation of the surface tension of silver with environment	5
Substrate heater	6
Shadow of a 10μ tungsten wire formed on a copper substrate at $\sim 450^\circ\text{C}$ by evaporating copper for two minutes	7
Step of silver formed by the evaporation of silver onto cleaved mica	8
Photographs of a step of silver on mica after heating at 480°C in air for 64 hours	9
The surface diffusion coefficient for silver in a vacuum of 5×10^{-6} torr 5×10^{-7} torr. Rhead's results in nitrogen plus 5% hydrogen and in vacuum are also shown	10
Surface self-diffusion coefficient for silver heated in air	11
Growth of the widths of grain boundaries with time for silver heated in air at 800°C	12
An example of the growth sequence when a film of silver on mica is heated in air at 360°C . Thickness of film $\sim 1100 \text{ \AA}$	13
A wedge shaped film of silver on mica after it has been heated at 300°C for 2 hours in air	14
Graphs of $(\text{final diameter of hole})^{5/2} - (\text{initial diameter of hole})^{5/2}$ against time interval for holes in a silver film of thickness 1.1×10^{-5} cm on mica when heated in air at 175°C	15 (a&b)
Graph of $(2r_f)^{5/2} - (2r_i)^{5/2}$ against time interval for a hole in a silver film of thickness 1.1×10^{-5} cm on mica when heated in air at 265°C	16 (a&b)
Graphs of $(2r_f)^{5/2} - (2r_i)^{5/2}$ against time interval for holes in a silver film of thickness 1.9×10^{-4} cm on mica when heated in air at 300°C	17
Graph of $\log D_s$ against $10^4/T$ for silver on mica heated in air	18
Silver films of thickness $\sim 1000 \text{ \AA}$ on mica and glass substrates after heating for $\frac{1}{4}$ hour at $\sim 300^\circ\text{C}$ in air	19 (a&b)
Graph of the diameter of a hole against estimated time since formation of hole for silver on mica at 265°C	20

1 INTRODUCTION

Few quantitative experiments have been performed to measure the mobility of atoms in evaporated deposits. Campbell¹ tried to measure the mobility of evaporated atoms by observing the penetration of evaporated atoms on a substrate into the umbra formed by placing a sharp edge between the source and substrate. The mobility was described in terms of the distance in which the thickness of the evaporated deposit fell to $1/e$ of its maximum value. He obtained values of this distance for evaporated gold on different substrates at room temperature which ranged from 1.2μ on carbon to 12μ on lithium fluoride.

Pashley et al² observed the coalescence of two small gold crystals into one on a substrate of molybdenum disulphide at 400°C . From the rate of growth of the neck between two crystals he deduced that a surface self-diffusion mechanism was the dominant process for the transfer of material but he did not attempt to obtain quantitative data.

The object of our exploratory experiments was to obtain, if possible, quantitative data on the mobility of metal atoms in metal films deposited by thermal evaporation on to various substrates, (later called "evaporated films"). Measurements were made of the mass transfer of material and as with all such experiments³ we obtained values of the product of the surface self-diffusion coefficient, D_s , and the surface energy, γ_s . In order to deduce D_s , it is necessary to assume values for γ_s .

The following methods were used to obtain D_s :-

- (1) the diffusion of evaporated material into the shadow cast by placing an object between the source and substrate, i.e. the smoothing of a step whose height is increasing at a constant rate;
- (2) the decay of the step produced by the evaporation of a metal layer on to a mica surface with cleavage steps;
- (3) the thermal grooving of grain boundaries; and
- (4) the growth of holes in a thin evaporated layer.

The grain boundary grooving method has been successfully applied previously to bulk silver⁴ and copper^{3,5}.

In these exploratory experiments the films were deposited in vacua of 10^{-5} to 10^{-6} torr. However these methods can also be used for clean surface experiments if ultra high vacua are used for the deposition and subsequent heating. Thus the successful use of evaporated films would make possible the

study of clean surfaces of the less refractory metals. These cannot easily be studied by the only other clean method of field emission³.

2 THEORY

The principles of the four methods are as follows:-

2.1 The decay of a step (Method 2)

When a metal is evaporated onto a mica surface with cleavage steps the contours of the mica are reproduced by the evaporated metal. The film thickness is arranged to be greater ($\sim 3000 \text{ \AA}$) than the step height ($\sim 2000 \text{ \AA}$), and sharp steps are selected. However, the method is restricted to metals which deposit epitaxially on the substrate and have the same crystal orientation on both sides of the step.

The step can smooth by surface diffusion, volume diffusion, viscous flow or the evaporation and condensation of metal atoms. For silver⁴ and copper⁵ below temperatures of 700°C it has been shown that surface diffusion is the dominant process in the grooving of grain boundaries for boundary widths less than about 20μ . We therefore assume that for step smoothing below 700°C where the characteristic widths are less than 20μ , surface diffusion is also the dominant mass-transfer mechanism. This argument also applies to the other methods used, when the characteristic dimensions of the region in which mass transfer is occurring is of order 20μ or less.

Mullins⁶ obtained for the smoothing by surface diffusion of a step $s(x, t)$ of initial height α situated at $x = 0$ after a time t

$$s(x, t) = \int_{-\infty}^x g(\epsilon, t) d\epsilon \quad (1)$$

where

$$g(\epsilon, t) = \frac{\alpha}{4\pi} \frac{1}{(Bt)^{\frac{1}{4}}} f\left[\frac{\epsilon}{(Bt)^{\frac{1}{4}}}\right], \quad (2)$$

$$f(u) = \sum_{n=0}^{n=\infty} (-1)^n \Gamma\left(\frac{2n+1}{4}\right) \frac{u^{2n}}{(2n)!}, \quad (3)$$

$$\begin{aligned}
B &= D_s \nu \Omega^2 \gamma_s / kT, \text{ and} \\
D_s &= \text{surface self-diffusion coefficient (cm}^2 \text{ sec}^{-1}\text{)} \\
\nu &= \text{surface density of atoms (cm}^{-2}\text{)} \\
\Omega &= \text{atomic volume (cm}^{-3}\text{)} \\
\gamma_s &= \text{surface free energy (dyne cm}^{-1}\text{)} \\
k &= \text{Boltzmann's constant (erg deg}^{-1}\text{)} \\
T &= \text{temperature } ^\circ\text{K.}
\end{aligned}$$

Using the fact that

$$\int_{-\infty}^0 g(\epsilon, t) d\epsilon = \alpha/2$$

and integrating the series obtained by substituting (3) and (2) in (1), we obtain for $s(x, t)$ the converging series

$$\begin{aligned}
s(x, t) &= \frac{\alpha}{2} + \frac{\alpha}{4\pi} \left[\Gamma\left(\frac{1}{4}\right) u - \Gamma\left(\frac{3}{4}\right) \frac{u^3}{3!} \right. \\
&\quad \left. + \frac{1}{4} \Gamma\left(\frac{1}{4}\right) \frac{u^5}{5!} - \frac{3}{4} \Gamma\left(\frac{3}{4}\right) \frac{u^7}{7!} + \dots \right] \quad (4)
\end{aligned}$$

where $u = \frac{x}{(Bt)^{\frac{1}{4}}}$. A plot of $s(x, t)$ is shown in Fig. 1. The abscissa is in terms of the dimensionless quantity $x / [(Bt)^{\frac{1}{4}}]$. Hence the distance from $x = 0$ (the initial position of the step) to the point where $s(x, t)$ first crosses the x axis is approximately equal to $2.3 (Bt)^{\frac{1}{4}}$. Since we did not observe the "hump and dip" on the sides of the step we take (see Section 5.3) the total "width" of the step to be

$$W \approx 4.6 (Bt)^{\frac{1}{4}} \quad (5)$$

2.2 Smoothing of a step whose height is increasing at a constant rate (Method 1)

If during evaporation an object with a sharp straight edge is placed between a source and substrate, and close to the substrate, a step is obtained whose vertical height increases at a constant rate, α . If the temperature of the substrate is hot enough to allow appreciable surface migration during deposition there will be a continual smoothing of the step as material diffuses into the umbra formed on the substrate by the object. In order that grain boundary grooving effects will not interfere with those due to step smoothing, deposition conditions must be such as to lead to large crystals.

In order to analyse the above situation we assume that the condensing atoms lose their excess kinetic energy on their first impact. Thus from

para.2.1, the solution $y(x,t)$ for the smoothing of the step edge is given by

$$y(x,t) = \int_0^t s(x,[t-t']) dt' \quad (6)$$

where $s(x,t)$ is defined by equation (1), α is replaced by α' and t is the total evaporation time. As we could not produce a converging series for this integral, a rough estimate of the width of the step sufficiently accurate for present purposes was taken to be $W \approx 4.6 (Bt)^{\frac{1}{4}}$ (as given in 2.1). This leads in principle, to an overestimate of D_s , but not by more than an order of magnitude.

2.3 Grain boundary grooving (Method 3)

If a polycrystalline specimen is annealed, grooves develop at the intersection of the grain boundaries with the surface. (This is due to the setting up of local equilibria.) For isotropic surface diffusion, with no loss of material into the grain boundary itself, a "hill" should develop on both sides of the groove, (Fig.2).

The grooves deepen with time and Mullins⁷ has shown that the groove width, w_s , is related to the time of anneal, t , by

$$w_s = 4.6 (Bt)^{\frac{1}{4}} \quad (7)$$

where $B = D_s v \Omega^2 \gamma_s / k T$.

For our experiments using this method the specimens consisted of polycrystalline silver films on mica. As for bulk materials, measurements are made only on those grain boundaries which do not move during annealing.

2.4 The growth of holes in thin evaporated films (Method 4)

Most work was done using this method. Given a suitable substrate on which the deposit can be formed with a sufficiently large crystal size, the subsequent heating will enable the film to reduce its surface area, by the creation and growth of holes. The motive force for the growth of an existing hole by surface diffusion is the surface tension. Consider the growth of a hole of radius r in an evaporated film of thickness d . We assume that the angle of contact of the film with the substrate at the edge of the hole is 90° and that, as the hole grows in size by surface migration, the cross-section of the edge of the hole is a "semi-circle" of radius x at any instant, (Fig.3). In practice small depressions are probably formed at the junction of the "semi-circle" and the undisturbed film but these are neglected. The flow of migrating surface atoms

is due to differences of chemical potential μ at regions of differing curvatures. Thus the net flux, j_s , of atoms at A along the surface is

$$j_s = - \frac{D_s}{kT} \frac{\partial \mu}{\partial s} \nu \quad (8)$$

where s is the distance along the metal surface, $s = 0$ being the point where the edge of the metal film surface joins the substrate. The surface concentration of atoms, ν , can be put equal to that of a flat surface if changes in μ are small with respect to kT .

If the solid is considered as bounded by a surface of uniform tension γ_s , then the pressure difference across the surface is $\gamma_s \left(\frac{1}{x} - \frac{1}{r} \right)$, whence the difference in chemical potential due to the surface tension, which is the Vdp term in the Gibbs free energy change, is

$$\begin{aligned} \mu_L - \mu_\infty &= - \Omega \gamma_s \left(\frac{1}{x} - \frac{1}{r} \right) \\ &= - \Omega \gamma_s / x \text{ for } r \gg x \end{aligned} \quad (9)$$

where the subscript L refers to equilibrium with the local surface, the subscript ∞ to equilibrium with a flat surface, and Ω is the atomic volume. Considering equation (8) and Fig. 3, we assume that the curvature changes from $\frac{1}{x}$ to zero within a distance πx . (This could be wrong by a factor of two or three.) Putting $\partial s = \pi x$ and $\partial \mu = \Omega \gamma_s / x$ in equation (8) we obtain

$$j_s = \frac{D_s \Omega \gamma_s}{k T \pi x^2} \nu \quad (10)$$

The total perimeter across which diffusion occurs is $2\pi r$, so that the volume rate of transfer of material, dV/dt , by surface diffusion is $j_s 2\pi r \Omega$. Hence

$$\frac{dV}{dt} = \frac{2 D_s \Omega^2 \gamma_s r}{k T x^2} \nu \quad (11)$$

Since the total volume of material is unaltered,

$$2\pi r \frac{\pi x^2}{2} = \pi r^2 d$$

or

$$\pi x^2 = r d \quad (12)$$

Hence substituting in equation (11) we obtain

$$\frac{dV}{dt} = \frac{2 D_s \Omega^2 \gamma_s \pi}{k T d} v \quad (13)$$

From Fig.4 we can see that $dV = 2\pi r \times dr$. Using equation (12) it follows that

$$\frac{dV}{dt} = 2\pi r \sqrt{\frac{rd}{\pi}} \frac{dr}{dt} \quad (14)$$

If we substitute for dV/dt using equation (14) in equation (13)

$$\begin{aligned} \frac{dr}{dt} &= \frac{D_s \Omega^2 \gamma_s v}{k T d r} \frac{1}{\sqrt{r d}} \\ &= \frac{B r^{-3/2} \pi^{1/2}}{d^{3/2}} \end{aligned}$$

Integrating gives

$$r^{5/2} = \frac{5 \pi^{1/2} B t}{2 d^{3/2}} \quad (15)$$

The merit of this method over the others is that we have a surface contour change whose time constant depends on film thickness. Thus for thin films ($< 3000 \text{ \AA}$), optically measurable changes occur in reasonably short times even for values of B and D_s , one or two orders of magnitude less than those producing measurable changes in practicable time intervals by the other methods.

2.5 The surface energy, γ_s

We used Method 1 for copper and Methods 2, 3 and 4 for silver. As all the above methods yield data on B (where $B = D_s v \Omega^2 \gamma_s / k T$) we need to assume a value for γ_s to obtain D_s . The values of γ_s used for copper in vacuo are those of Udin⁸ given by the equation

$$\gamma_s = 2445 - 0.5875 T \text{ ergs/cm}^2$$

where T is the temperature in degrees absolute.

The values of γ_s used for silver are shown in Fig.5. Those in air are by Buttner et al⁹ and those in purified helium by Funk et al¹⁰. From the data given for the adsorption of oxygen on silver in Section 5.4 it can be shown that oxygen adsorption should take place ($\theta \geq \frac{1}{2}$) for $P_{O_2} \geq 10^{-5.3}$ atmospheres at

930°C. From the graph given by Buttner et al⁹ for the oxygen partial pressure dependence of the surface energy of solid silver at 932°C it can be seen that, extrapolating to a P_{O_2} of $10^{-5.3}$ atmospheres we obtain the γ_s quoted for purified helium. This means that the values of γ_s we quote for purified helium are for silver free from adsorbed oxygen and can be used for γ_s in a vacuum if no adsorbed layer is present. It can be seen from Fig.5 that discrepancies arise from extrapolating the results for γ_s to low temperatures as the two curves cross at a higher temperature than absolute zero. As we were primarily concerned with the order of magnitude of D_s in our experiments, γ_s for silver in air at 200°C to 400°C was taken to be equal to that for silver in helium. (This gives an upper limit to γ_s .)

3 EXPERIMENTAL

The evaporation experiments were done in a vacuum unit with a pressure of $\sim 5 \times 10^{-6}$ torr before evaporation and of $\sim 5 \times 10^{-5}$ torr during evaporation. This unit consisted of a glass belljar of 12" diameter by 14" high sealed to a mild-steel baseplate with a L-shaped viton gasket, a baffle valve, liquid nitrogen trap and a F203 diffusion pump backed by a rotary pump. Current and rotary feed-throughs were sealed to the baseplate using "O" rings. The rotary feed-through was used to operate a shutter placed between the substrate and the evaporation source. Thermocouple feed-throughs were made by brazing ceramic-metal feed-throughs into a mild steel "blanking off" plate.

The evaporation source was a molybdenum boat 0.15 cm wide, 3.5 cm long and 0.6 cm deep heated by radiation from a U-shaped tantalum strip which surrounded it. To reduce the heating of the belljar and contents, the source was surrounded by three cylindrical heat shields. The evaporated beam passed through a slit onto the substrate. The distance from source to substrate was 8 cm.

The copper charge for the boat was "spectrographically standardised" copper wire, supplied by Johnson, Matthey and Co. Ltd., which had been surface cleaned by electropolishing in a bath of orthophosphoric acid (density 1.38 gm/cc) using procedures similar to Mullins and Shewmon¹¹. It was then washed in 10% by volume of orthophosphoric acid (density 1.75 gm/cc) to minimise phosphate residue, distilled water, and Analar Acetone. The "spectrographically standardised" silver wire charge was cleaned by dipping it in concentrated nitric acid, then washed in boiling distilled water, cold distilled water and methyl alcohol and then dried. The temperature of all charges was slowly brought up to the evaporation temperature and retained at this for at least one minute to outgas before the molybdenum shutter was opened and the deposition started.

Two substrate heaters were used in these experiments. The larger power heater consisted of a $\frac{1}{4}$ " thick copper block of surface size $\frac{1}{2}$ " \times $1\frac{1}{2}$ ". Heating elements of platinum-13% rhodium wire in 2 mm diameter pyrex tubes and two thermocouples were inserted into holes drilled parallel to the substrate heating surface. The specimens were clamped to the heater by a copper plate. The other heater consisted of a piece of tantalum strip, 0.004 inches thick and approximately a quarter of an inch wide, bent as shown in Fig.6. The strip was heated directly by passing a current through it and its temperature was measured by thermocouples welded on to its back surface. The temperature of the deposit was no doubt slightly different from that given by the thermocouple and it was estimated that the temperature difference was probably less than 10°C. The substrates were clamped to this heater with small tantalum strips. The former heater was used in the experiments using Method 1 and the latter in the other methods.

4 THE SMOOTHING OF A STEP WHOSE HEIGHT IS INCREASING AT A CONSTANT RATE (Method 1)

4.1 Introduction

This was the first method used. The surface self-diffusion of copper by grain boundary grooving with bulk specimens has been studied earlier⁵ and thus comparable data on evaporated copper films was of interest.

Since the use of a mica substrate to produce epitaxial films of copper is difficult, it was decided to try copper itself as a substrate and to work at high temperatures in order to produce a suitably large crystal size. The experiment was one of simultaneous deposition and diffusion and, despite the resulting difficulties in analysis, served to show if the system was worth studying further. It was one which can easily be repeated under clean conditions in ultra-high-vacua.

4.2 Experimental

The shadow step was produced by clamping 10 μ (and 90 μ) diameter tungsten wires across the specimen using the same copper clamping plate as was used to hold the specimen itself.

To reduce the width of the penumbra, the wires were parallel to the long dimensions of the boat; for the 10 μ wire the penumbra was 0.1 μ wide. Thus significant experimental results require a half width of the step after smoothing of \gg 0.1 μ . The previous work⁵ indicated that, to obtain smooth step widths of $d \sim 2\mu$ with copper in vacuo, high temperatures ($>450^\circ\text{C}$) or impossibly long evaporation times would be required.

15

Bulk copper specimens 1.5 cm by 0.5 cm by 0.05 cm were used as a substrate. The copper was annealed to give a large grain size, then prepared by electro-polishing and washing as described previously for the copper charge (Section 3). In order to promote rapid cooling of the substrate as soon as the experiment was completed the apparatus was let down to atmospheric pressure with dry nitrogen. 18 minutes were required for the substrate to cool from 600°C to 100°C.

After evaporation the specimens were examined with a "Hilger and Watts" interference microscope and the widths of the steps were measured using a micrometer eyepiece. The region of minimum width along the whole length of the shadow was selected as being the point where the wire touched the substrate and therefore the region with minimum uncertainty due to penumbra. The pressure during these experiments was of order 10^{-5} torr.

4.3 Results

It was found that the type of evaporated film obtained depended on the orientation of the substrate grain. Some of the evaporated material was produced in a granulated form (Fig.7). With such films it was more accurate to use a graduated eyepiece than to measure a photograph. The width of the steps varied suddenly from one substrate grain to the next and also from side to side of the wire showing a large orientation dependence of D_s ; the maximum width of the step corresponded to the substrate grains with the smallest grain size of deposit. The maximum observed diffusion coefficients for copper were of order 10^{-6} cm²/sec at 450°C and 10^{-5} cm²/sec at 600°C. The minimum diffusion coefficients obtained were $\sim 1/15$ of these.

4.4 Discussion

These experiments did not give better than an order of magnitude estimate of D_s due to the approximations used in the analysis and to the large thermal inertia of the heater which caused cooling times comparable with the time of the experiment. The authors⁵ previous experiments with bulk copper in a vacuum of $\sim 1 \times 10^{-7}$ torr gave a D_s at 600°C of $(2.5 \pm 0.5) \times 10^{-6}$ cm²/sec and at 450°C of $(3.5 \pm 0.8) \times 10^{-7}$ cm²/sec. Because of the large spread in widths of the shadow step obtained in these experiments it can only be seen that the order of D_s 's are the same for the two experiments. This means that within the rather poor accuracy of the method the surface mobility of atoms immediately after deposition by evaporation is the same as for surface atoms of the bulk material.

5 THE DECAY OF A STEP (Method 2)

5.1 Introduction

In view of the difficulties experienced with copper films, the system of silver on mica¹² was used for this method. The bulk surface diffusion of silver had previously been measured by Rhead⁴, and so comparative data on evaporated films was again of interest.

Pashley¹² found that if silver was evaporated at a rate of 10 Å/sec on to cleaved mica heated to a temperature between 250°C and 300°C, a well orientated single crystal could be obtained when the silver reached a thickness of 1000 Å. The orientation he found was {111} Ag // {001} mica cleavage and $\langle \bar{1}10 \rangle$ Ag // to $\langle 010 \rangle$ mica. By using these conditions a single crystal of silver was produced on mica in which there was no change in orientation across the step. However, in our experiments the mica step heights were about 2000 Å, and thicknesses > 3000 Å were required to ensure continuity of the silver film. Using the Pashley method to produce such thick films gave a crystal size which was too small to prevent grain boundary grooving interfering with step smoothing. We therefore used the modified method of Lowe¹³ in which films of ~ 1000 Å are deposited on to a substrate at 280°C at a rate of ~ 20 Å/sec and then growth continued at an increased substrate temperature of 400°C and at an increased evaporation rate. In this way a large crystal size was obtained in the required film thickness. Its orientation is similar to Pashley's, i.e. {111} Ag // {001} mica cleavage plane $\langle \bar{1}10 \rangle$ Ag // $\langle 010 \rangle$ mica.

5.2 Experimental

The mica substrates were cleaved in air and quickly transferred to the evaporation unit described in Section 3. The thicknesses of the films were measured with an interference microscope. Since mica is soft, a pyrex strip was also used as a substrate in some experiments so that the thicknesses of the evaporated films could be checked with a Talysurf. The pyrex strips were prepared by washing them in RBS 25 detergent (manufactured by "Medical Pharmaceutical Developments Ltd.) rinsing in boiling distilled water, then methyl alcohol and then heating them overnight at 300°C in air. An example of the steps produced is shown in Fig.8. Such steps were annealed for a measured time in either air or a vacuum.

5.2.1 Vacuum anneals

Since the substrate heater used in the preparation of silver steps on mica did not allow very accurate temperature measurement and the pressure in the evaporation chamber was not less than 5×10^{-6} torr we transferred the

specimens to another vacuum furnace operating at 5×10^{-6} to 3×10^{-7} torr for the diffusion experiments. This furnace was a glass system which enclosed a silver boat and lid containing the specimens, and was pumped by a silicone oil diffusion pump via a liquid-nitrogen trap. The specimens were put in the silica tube through a viton "O" ring seal. A furnace was drawn over the silica tube during anneals. Temperatures were measured by an external thermocouple.

5.2.2 Air anneals

For the anneals in air the specimens, contained in a silver boat, were placed in an open-ended silica tube which was put into a furnace whose temperature was measured by thermocouples. The change in width of the evaporated step with time of heating was measured using a micrometer eyepiece on a Hilger and Watts interference microscope.

5.3 Results

An example of the resulting shape of the steps after annealing is shown in Fig.9. The hump and dip theoretically predicted and shown in Fig.1 were not observed. This may be because the predicted height for the hump and dip was only 5% of the total height of the step and therefore too small to be seen. At high temperatures some of the step profiles had a small ridge instead of hump on one side. As this may have been due to the stepped mica separating from the sheet (due to the evolution of water at high temperatures) it was decided to work at lower temperatures. In some of the experiments the face of the step did not remain smooth; this may have been due to the presence of adsorbed oxygen causing faceting.

The values of D_s obtained by the analysis of the decay of a silver step in a vacuum of approximately 5×10^{-6} torr using γ_s for a clean surface (Fig.5) are shown in Fig.10. Rhead's⁴ results using grain boundary grooving in bulk materials to obtain the D_s of silver in a vacuum of 5×10^{-7} torr and his results in an atmosphere consisting of nitrogen plus five per cent molar concentration of hydrogen at a minimum dew point of -78.5°C are shown for comparison. The thickness of most of the films used were in the range 2000 Å to 4000 Å and the step heights were in the range 1250 Å to 3000 Å.

The measured D_s for silver in vacuo (see Fig.10) was small ($D_s \approx 2 \times 10^{-7}$ cm²/sec at 700°C) and of the order of the limit of detection. In order to investigate the method further, lower temperature experiments on step smoothing were therefore done in air since it was expected that the presence of oxygen would increase the apparent surface diffusion coefficient. This proved to be so and surface mobility was observed at 480°C with $D_s \approx 1.5 \times 10^{-7}$ cm²/sec. The

values of D_s obtained from the analysis of the smoothing of silver steps in air are shown in Fig.11. Rhead's⁴ results, using grain boundary grooving in bulk silver, are also shown for comparison. Rhead could not measure the growth of grain boundaries below 700°C as extensive faceting occurred.

5.4 Discussion

Oxygen is readily adsorbed on the surface of silver and because of the high heats of adsorption involved it is generally accepted that oxygen is adsorbed as atoms. The reaction can be represented as



where (Ag - O) represents an oxygen atom adsorbed on a surface site. Then

$$\Delta G = \Delta H - T\Delta S = - R T \ln \left[\frac{\theta^2}{P_{O_2} (1 - \theta)^2} \right]$$

where ΔG , ΔH and ΔS are the free energy, enthalpy and entropy of adsorption, θ is the fractional surface coverage and P_{O_2} is the oxygen pressure in atmospheres. Gonzalez and Parravano¹⁴ obtained, for small θ , $\Delta H = -108$ Kcal/mole of oxygen and $\Delta S = -66$ cal/mol/degree. This indicates that oxygen adsorption should take place ($\theta \approx \frac{1}{2}$) for $P_{O_2} \approx 10^{-4.7}$ torr at 800°C.

In our vacuum experiments we were working in a pressure $\approx 5 \times 10^{-6}$ torr with residual gases probably tending to reduce θ rather than increase it. This means at this pressure and at a temperature of 800°C the coverage θ for oxygen $\ll 1/10$. The same argument could reasonably apply to Rhead's results in vacuo and the oxygen adsorption in his nitrogen-plus-hydrogen atmosphere should have been even less. It is not clear why his experiments in the two environments which he used gave different results above 800°C, but our own measurements in vacuo agree reasonably well at 800°C with his in nitrogen-plus-hydrogen. At lower temperatures it is possible that oxygen adsorption in our vacuum conditions would lead to values of D_s greater than Rhead's in nitrogen-plus-hydrogen.

Our results for the surface self-diffusion of silver in air (see Fig.11) when extrapolated intersect those of Rhead at 800°C, but, at 600°C and below, the values we obtain for D_s are slightly higher than those expected from the extrapolation to 600°C of Rhead's results to lower temperatures. This may be due to the fact that as the temperatures of the experiments are reduced and spread obtained in D_s increases (see spread in Rhead's values in Fig.11) and, as we have picked mainly {111} planes by evaporating silver on mica, we may have picked a particular plane which corresponded to the upper values in Rhead's

scatter. Choi and Shewmon¹⁵, studying thermal grooving of copper in hydrogen found that D_s for {111} planes was larger than that for {110} and {100}, the ratio $D_s\{111\}/D_s\{100\}$ having a mean of 2.8. Blakely and Mykura¹⁶ using the decay of a scratch on bulk nickel in a vacuum of 10^{-4} torr also found that D_s was greater near the {111} plane. As Blakely and Mykura probably had oxygen adsorbed on their nickel it appears that, for both clean f.c.c. metals and f.c.c. metals with adsorbed oxygen surface diffusion is faster near the {111} plane.

6 GRAIN BOUNDARY GROOVING IN EVAPORATED DEPOSITS (Method 3)

6.1 Introduction

As the slight difference between our results and Rhead's⁴ could be due to the method of measuring D_s by the smoothing of evaporated steps it was decided to check our values for D_s by making some measurements on the growth in air of grain boundaries in evaporated silver.

6.2 Experimental

If Pashley's and Lowe's evaporation conditions (see 5.1) are slightly altered, by using either higher substrate temperatures or different evaporation rates, Pashley has shown, and we confirm, that the desired polycrystalline film results. Such polycrystalline films were annealed in air as described in Section 5.2.2. In practice, grain boundary grooving experiments were carried out at the same time as the smoothing of evaporated steps. The change in width of the grain boundary grooves with time after heating was measured, as before, with the interference microscope.

6.3 Results

The values of D_s obtained from the analysis (2.3) of the grain boundary grooving of evaporated silver in air together with previous results are shown in Fig.11. On drawing the curve most weight was placed on the values for D_s at 800°C ($10^4/T = 9.3$) and 600°C ($10^4/T = 11.45$) as these are the average results from at least 6 grooves. Fig.11 shows that there is very good agreement between the values of D_s obtained from the smoothing of an evaporated step and from the growth of a grain boundary in evaporated films. As an example of the growth rates observed, a plot of the widths of the grain boundary grooves against time at 800°C is shown in Fig.12. Each point on the graph is the average width of at least six grain boundaries. (The bars show the total spread in the actual values of width.) The resulting line of best fit (Fig.12) represents a line which approximates well to the $t^{1/4}$ law expected from the analysis giving support to the assumption that the mass transport was due to surface diffusion. As 800°C was the highest temperature used for these experiments it was even more likely that

surface diffusion was the dominant mechanism at low temperatures. However the shapes of the grain boundary grooves found in these experiments were not the same as those expected from Mullins⁷ analysis and shown in Fig.2 as they did not have such distinct humps on each side of the grain boundary. Rhead also observed this in his experiments on silver in nitrogen-plus-hydrogen. Loss of material down the grain boundary or possibly anisotropy of surface diffusion may account for this.

6.4 Discussion

The good agreement between diffusion data from step smoothing and grain boundary grooving in air leads us to suggest that our earlier comparison (Section 5.4) of step smoothing results in vacuo with Rhead's data from grain boundary grooving in vacuo and nitrogen-plus-hydrogen was reasonable.

The values of D_s , from grain boundary grooving in air, are again greater than those of Rhead's⁴ and the reasons given in Section 5.4 may also apply here.

7 THE GROWTH OF HOLES IN THIN EVAPORATED FILMS (Method 4)

7.1 Introduction

When evaporated films of silver, of thickness less than approximately 3000 Å, on mica are heated, in air, holes are nucleated in the film and grow with time.

Let us consider equation (15), i.e. $r^{5/2} d^{3/2} = 2.5 \pi^{1/2} Bt$. If the radius of the hole, r , is equal to the thickness of the film, d , we obtain $r^4 = 2.5 \pi^{1/2} Bt$. If we compare this with the equation for the growth of a grain boundary $w_s = 4.6 (Bt)^{1/4}$ (7) and if we set the same observable limit (i.e. 1 μ) on the order of the width, w_s , of the grain boundary groove and the diameter of a hole 2 r , it can be seen that the smallest B , and therefore D_s , observable is the same in each case. However if we choose a film thickness much less than 1 μ the observable B and D_s can be decreased by at least an order; (two orders would require a film thickness of approximately 500 Å).

Two limits were placed on the temperature of the experiment. Above approximately 300°C mica releases water vapour and a lower limit of about 175°C was set by the very long time the holes took to nucleate in air. Film thicknesses were chosen so as to produce, on subsequent heating, discrete holes of greater than 1 μ diameter. (1 μ being the practical lower limit for our optical measurements of hole sizes.) Within these limits, we were unable to nucleate holes in silver films in vacuo, though we were able to observe hole growth.

7.2 Experimental

Single crystal silver films on mica were made as described in Section 5.1. The silver was also evaporated on to pyrex (prepared as described in 5.2) at the same time in order to compare the behaviour of the two films on annealing in a vacuum and in air. The thicknesses of the silver films varied from 270 Å to 10^4 Å. Some films were also made in the form of wedges of maximum thickness 7500 Å by putting a mask at such a distance from the substrate as to produce a suitable penumbra. The change in the appearance of the films with time after heating (method described in 5.2.1 and 5.2.2) was recorded using a standard photo-micrographic method. As it was hoped to lower the order of magnitude of D_s measurable by this method all anneals were in the temperature range 175°C to 375°C which was below the range of previous measurements made by grain boundary grooving methods.

7.3 Results

We will consider first those results obtained from heating in air, since here the break up of the film into holes was rapid. The complete nucleation, growth and break up to produce channels with final shrinking of the film into globules is shown in Fig.13.

The change in the appearance of the films on heating in air produced by changing the thickness of the silver films on mica is shown in the wedge film in Fig.14. The thickness of this film varied from zero to 2700 Å. It can be seen that it contained holes at ~ 2300 Å thickness, channels at ~ 1800 Å, and formed globules at 900 Å. As expected the thicker the silver film, the slower was the nucleation and growth of holes and the larger the holes were before the channel "stage" occurred. In addition the globules finally formed were larger with a thick film. Little reliability can be placed on the absolute thicknesses of the wedge film quoted due to the non-linearity of the decrease in thickness of the wedge. No measurements were made using wedge films.

Equation (15) gives the relation between the radius, r , of the hole and the time, t , since the start of the hole formation. Since the start is never clearly observed, our analysis for D_s is based on measurement of the radii of the hole, r_f and r_i , at times t_f and t_i respectively. The subscripts f and i refer to final and initial observations. The variation of $(2r_f)^{5/2} - (2r_i)^{5/2}$ with $t_f - t_i$ should be linear. Figs.15, 16 and 17 show such plots for experiments at 175°C, 265°C and 300°C. No plots are shown for experiments at 360°C since the film agglomerated so quickly that only two points were obtained. These graphs show that the theory proposed in Section 2.4 applies to the growth

of the holes. From the slopes of the lines in Figs. 15, 16 and 17, values of D_s were obtained and are shown in Fig. 18. The cross-section of the film edge as shown in Fig. 4 was not always seen. In practice there was sometimes a flattening of the ridge producing a plane parallel to the substrate.

Similar films were made on pyrex glass substrates and were heated in air. For an equal thickness ($\sim 1000 \text{ \AA}$) the film on glass broke up into a structure which was much finer than that on mica (Fig. 19). This is to be expected since without epitaxy the film was probably polycrystalline on a very fine scale.

Attempts were made to do similar experiments in vacuo of $\sim 10^{-6}$ torr on films of $\sim 1000 \text{ \AA}$. However after heating to 400°C for 74 hours, no changes could be seen on either pyrex or mica substrates. Either there was a difficulty in hole nucleation or the diffusion coefficient was much less. To overcome the nucleation difficulty and obtain a ratio for D_s in air to that in vacuo, holes were nucleated and grown in air and then transferred to vacuum for observation of any further growth. The result of such an experiment is shown in Fig. 20. From the analysis in Section 2.4

$$D_s \propto \frac{(2r_f)^{5/2} - (2r_i)^{5/2}}{t_f - t_i}$$

If we had left the hole represented in Fig. 20 of diameter $2r_i = 2.1 \mu$ to grow in air it would have reached a diameter $2r_f$ [air] of approximately 7.4μ in $167\frac{1}{4}$ hours, whereas in a vacuum of $\sim 10^{-6}$ torr it actually reached a diameter $2r_f$ [vac] of 2.35μ in the same time. Therefore the ratio

$$\frac{D_s \text{ in air}}{D_s \text{ in vacuum}} \text{ at } 265^\circ\text{C} = \frac{(2r_f[\text{air}])^{5/2} - (2r_i)^{5/2}}{(2r_f[\text{vac}])^{5/2} - (2r_i)^{5/2}} = \frac{7.4^{5/2} - 2.1^{5/2}}{2.35^{5/2} - 2.1^{5/2}}$$

$$\approx 70$$

If the line of best fit of the points in Fig. 20 is extrapolated to give $2r_f$ air rather than the $t^{2/5}$ line the ratio obtained is ≈ 150 , so that as a rough guide, we can say that D_s for silver in a vacuum is at least two orders smaller than in air at 265°C . Further experiments of this type are needed at temperatures between 265°C and 700°C to demonstrate the use of this method for measuring small values of D_s .

7.4 Discussion

The values for D_s of silver in air from the growth of holes at low temperatures are much larger than those obtained by extrapolating the values for D_s shown in Fig.11 to lower temperatures. The theory proposed in section 2.4 gave a growth law which seems to fit our results as the slopes of both our graphs in Fig.18 and Fig.11 are the same within experimental scatter. Therefore formula (15) may only be wrong in its constant. Given that the value of D_s at 265°C in vacuo is approximately two orders lower than that in air then it can reasonably be concluded that this alone was not responsible for our failure to see the holes in vacuo but that there must have been an additional factor in the nucleation stage.

8 CONCLUSIONS

Using mass-transfer methods, the order of the surface self-diffusion coefficient, D_s , of silver and copper has been found to be independent of whether the metal is in a bulk or evaporated film form. It has also been shown that an increase of oxygen pressure increases the surface diffusion rate of silver.

The above experiments have also demonstrated that D_s can be measured using the new techniques of step smoothing and hole growth in evaporated deposits. The growth law for a hole viz: "the radius of a hole, r , growing by surface diffusion is proportional to $t^{2/5} d^{-3/5}$ where t is the time since the formation of the hole and d the thickness of the film", was proposed and verified experimentally. Using this method, D_s 's of two orders of magnitude lower than that calculated from any of the other methods were measured. The difficulties of nucleating holes in vacuo would be an obstacle to carrying out a complete evaporation and diffusion experiment in ultra high vacua (at least with silver or mica), but more experiments could be done in which holes are nucleated by heating evaporated silver films in air and then grown at temperatures between 265°C and 700°C in a vacuum. However lack of time prevented this most obvious extension of the work and a more detailed confirmation of the observations made.

Acknowledgement

We wish to thank D. M. Gilbey for his help with the theories proposed in Section 2.

SYMBOLS

D_s	=	surface self-diffusion coefficient ($\text{cm}^2 \text{sec}^{-1}$)
γ_s	=	surface free energy (erg cm^{-2})
a	=	step height (cm)
ν	=	surface density of atoms (cm^{-2})
Ω	=	atomic volume (cm^3)
k	=	Boltzmann's constant (erg deg^{-1})
T	=	temperature ($^{\circ}\text{K}$)
α^{\dagger}	=	rate of which a step height is increasing (cm sec^{-1})
w_s	=	width of grain boundary due to surface diffusion (cm)
W	=	width of a step due to surface diffusion (cm)
t	=	time of anneal (sec)
$t_f - t_i$	=	time interval for a hole's radius to increase from r_i to r_f (sec)
r	=	radius of a hole (cm)
r_i	=	initial radius of a hole (cm)
r_f	=	final radius of a hole (cm)
d	=	thickness of a film (cm)
j_s	=	net flux of atoms along a surface
μ	=	chemical potential of atoms (erg)
ΔH	=	enthalpy of adsorption (k cal per mole)
ΔS	=	entropy of adsorption (cal per mole per degree)
θ	=	fractional surface coverage of oxygen

<u>No.</u>	<u>Author</u>	<u>Title, etc.</u>
1	D. S. Campbell	Trans. 9 th Vacuum Symposium, 29, (1962)
2	D. W. Pashley	Phil. Mag. 10, 127 (1964)
	M. J. Stowell	
	M. H. Jacobs	
	T. J. Law	
3	J. M. Blakely	Progress in Materials Science, Published Pergamon Press 10, (1963)
4	G. E. Rhead	Acta Met. 13, 223, (1965)
5	F. J. Bradshaw	Acta Met. 12, 1057, (1964)
	R. H. Brandon	
	C. Wheeler	
6	W. W. Mullins	J. Appl. Phys. 30, 77, (1959)
7	W. W. Mullins	J. Appl. Phys. 28, 333, (1957)
8	H. Udin	Metal Interfaces, Published A.S.M. 114, (1951)
9	F. H. Buttner	J. Phys. Chem. 56, 657 (1952)
	E. R. Funk	
	H. Udin	
10	E. R. Funk	Metal Interfaces, Published A.S.M. 122, (1951)
	H. Udin	
	J. Wulff	
11	W. W. Mullins	Acta. Met. 7, 163, (1959)
	P. G. Shewmon	
12	D. W. Pashley	Phil. Mag. 4, 316, (1959)
13	R. M. Lowe	Acta. Met. 12, 1111, (1964)
14	O. D. Gonzalez	J. Am. Chem. Soc. 78, 4533, (1956)
	G. Parravano	
15	J. V. Choi	Trans. A.I.M.E. 224, 589, (1962)
	P. G. Shewmon	
16	J. M. Blakely	Acta. Met. 9, 23, (1961)
	H. Mykura	

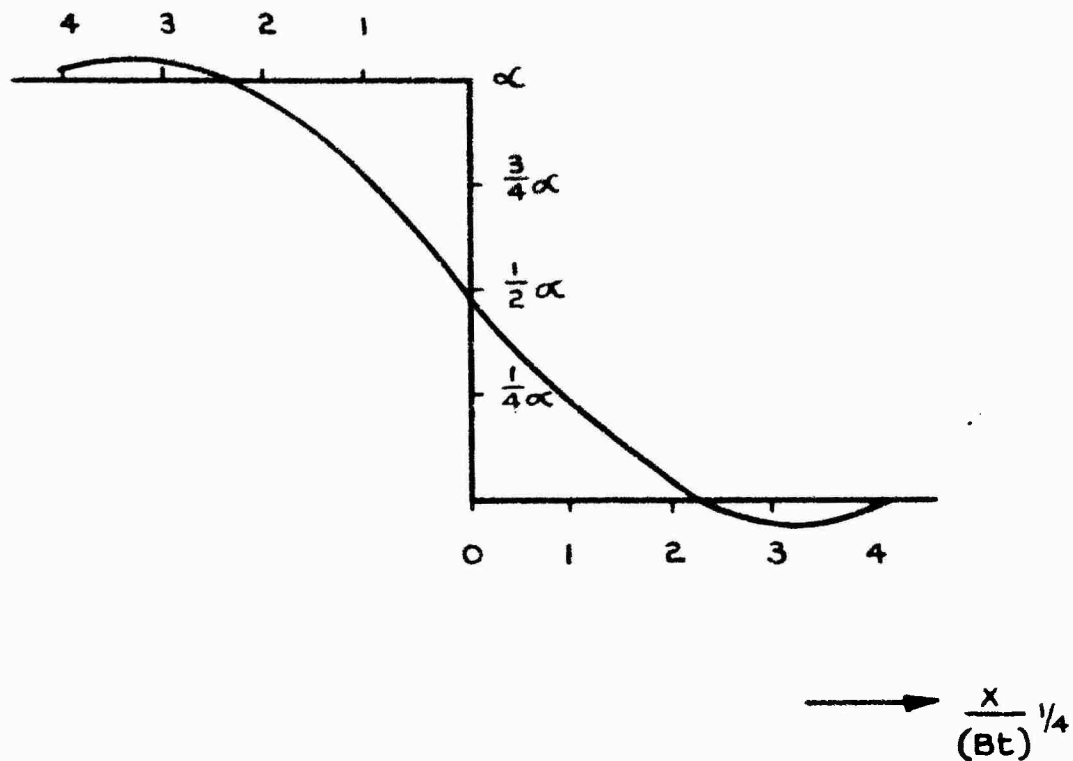


FIG. 1. THE SMOOTHING OF A STEP OF HEIGHT α ,
DUE TO SURFACE DIFFUSION

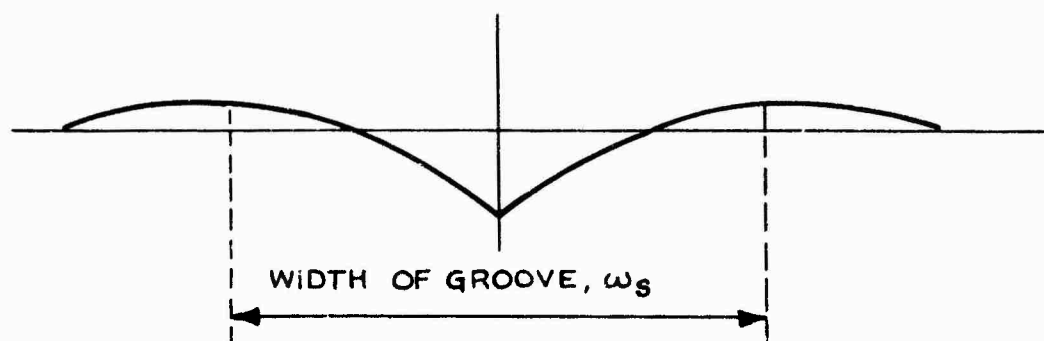


FIG. 2. THE SHAPE OF A GRAIN BOUNDARY GROOVE
DUE TO SURFACE DIFFUSION

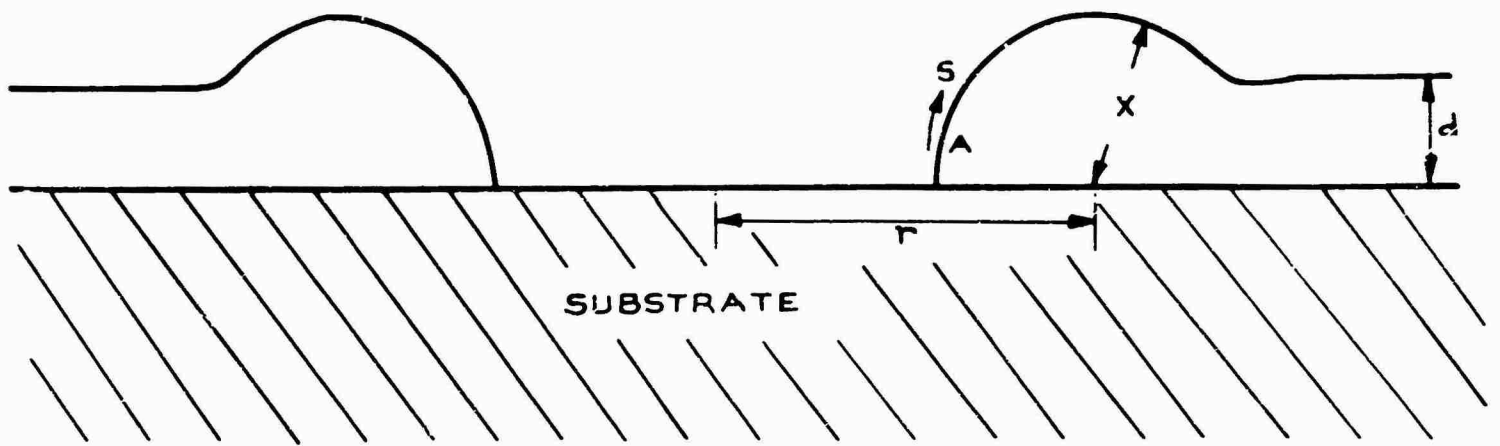


FIG.3. THE PROFILE OF A HOLE IN AN EVAPORATED FILM WHICH IS GROWING BY SURFACE DIFFUSION (NOT DRAWN TO SCALE)

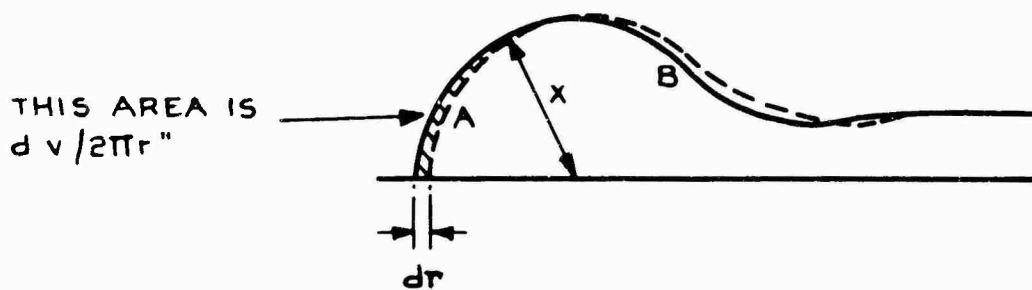


FIG. 4. PROFILE OF HOLE EDGE

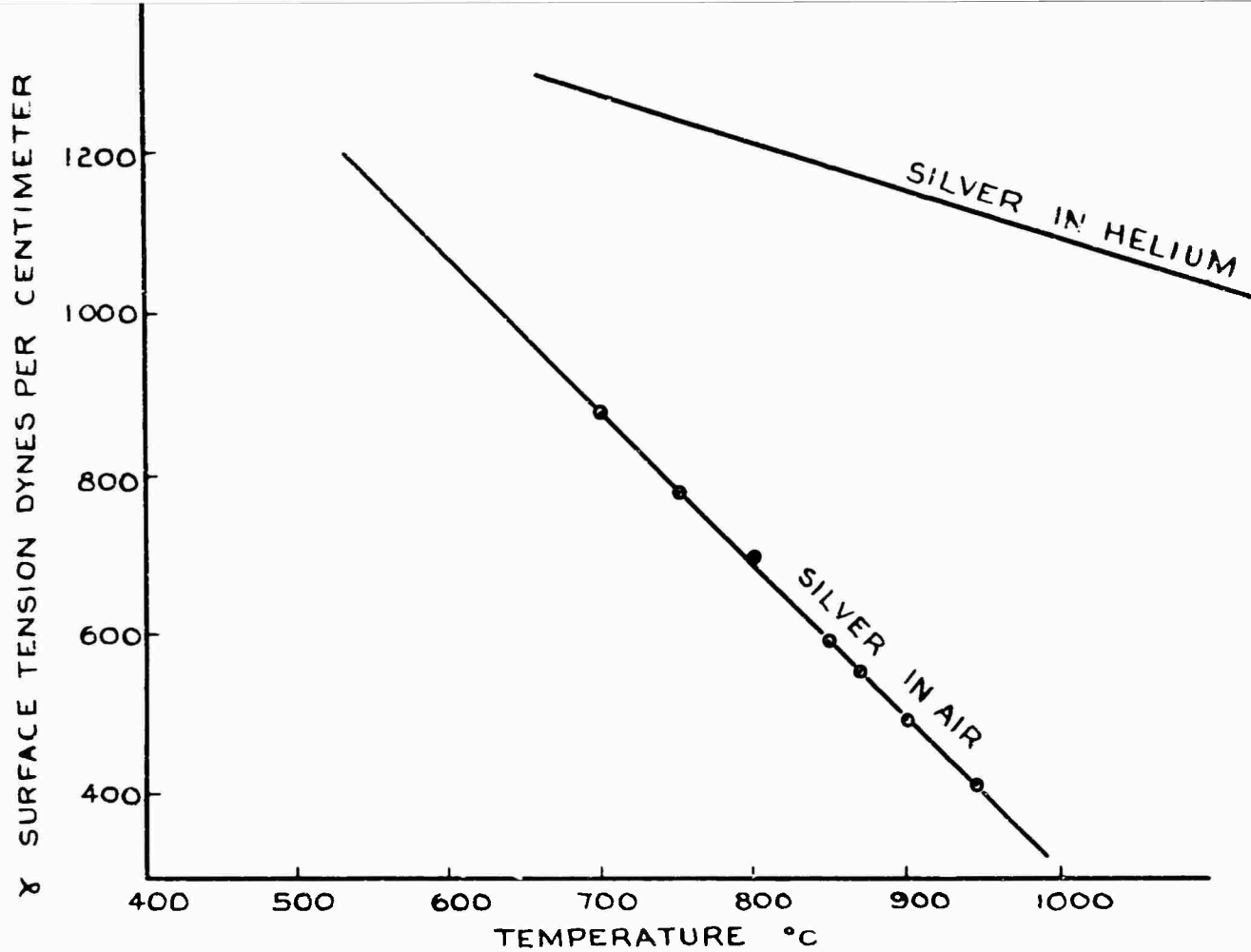


FIG. 5. THE VARIATION OF THE SURFACE TENSION OF SILVER WITH ENVIRONMENT

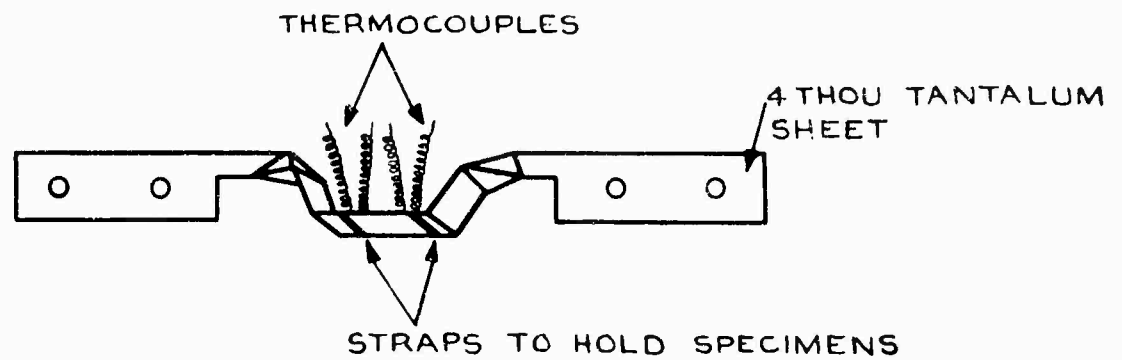


FIG. 6. SUBSTRATE HEATER

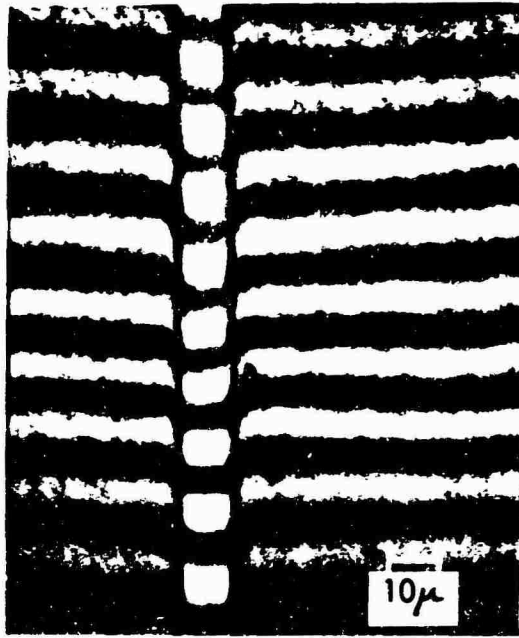


Fig.7. Shadow of a 10μ tungsten wire formed on a copper substrate at $\approx 450^{\circ}\text{C}$ by evaporating copper for 2 minutes

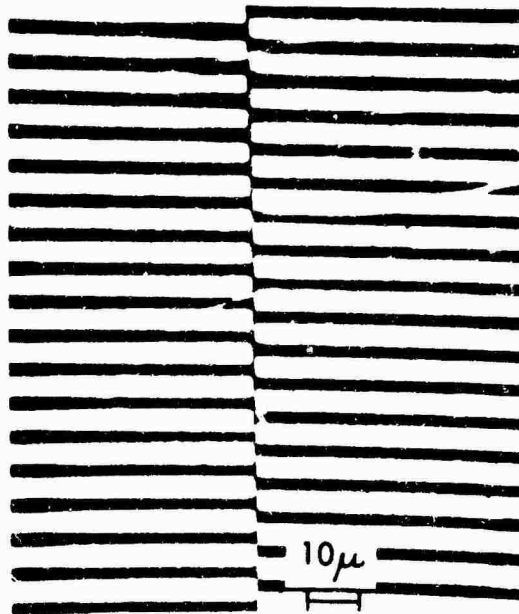


Fig.8. Step of silver formed by the evaporation of silver on to cleaved mica

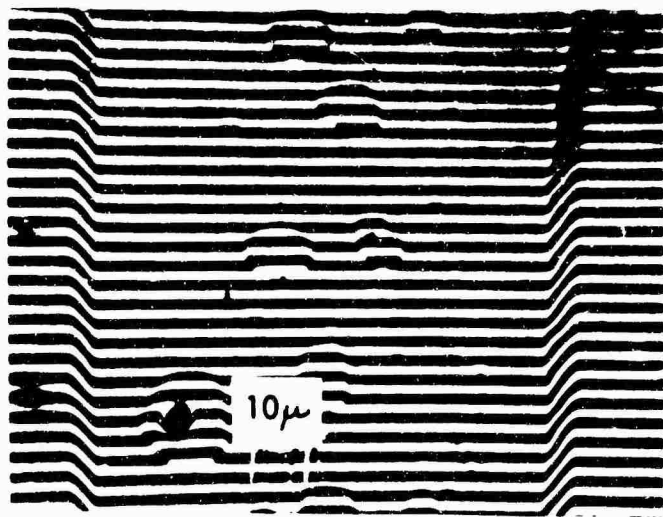
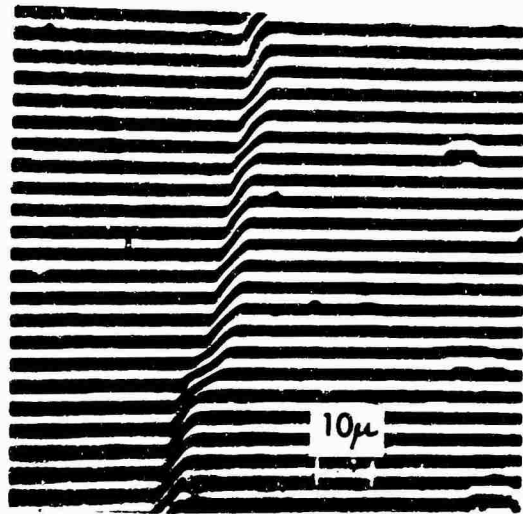


Fig.9. A step of silver on mica after heating at 480°C in air for 64 hours

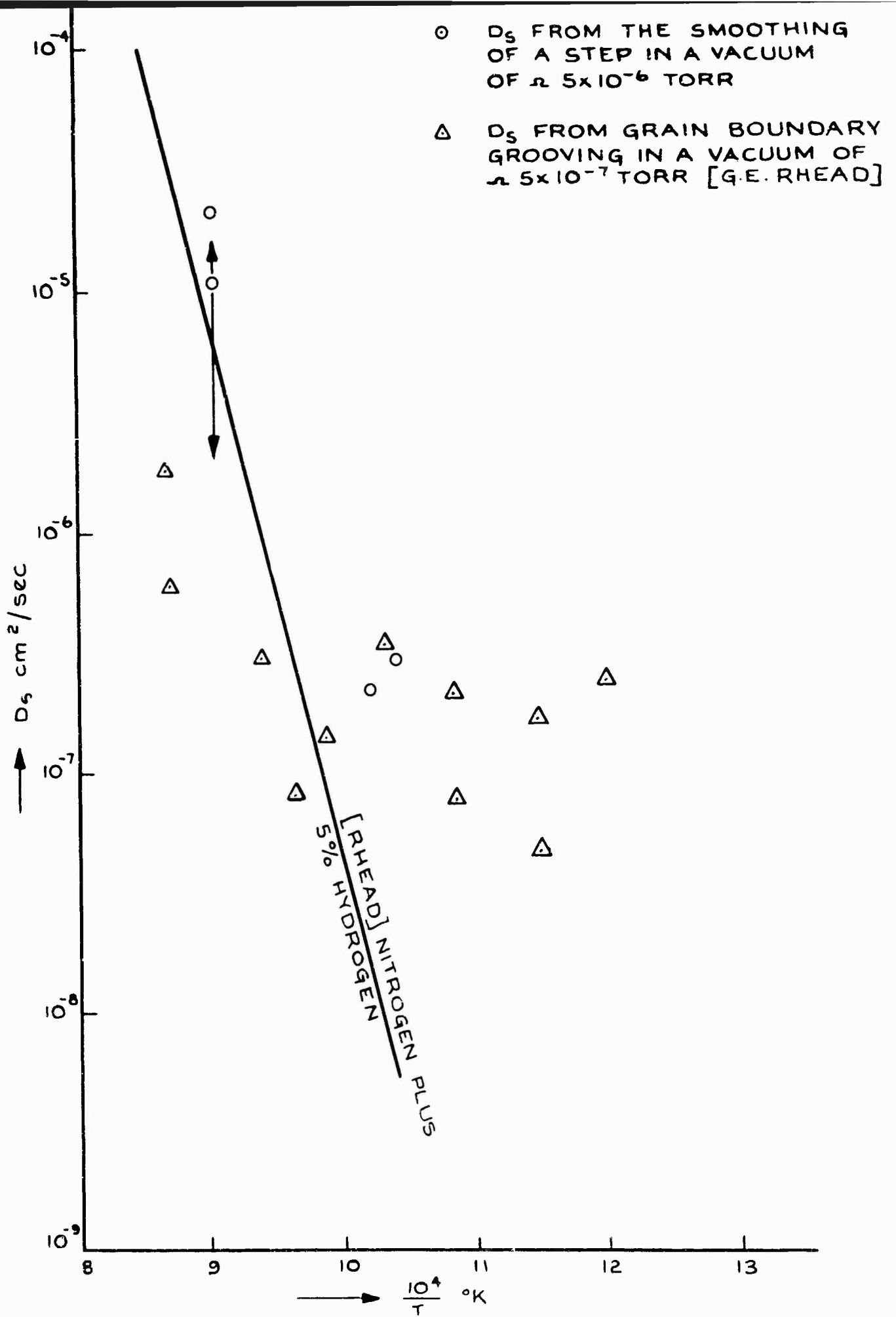


FIG 10 THE SURFACE DIFFUSION COEFFICIENT FOR SILVER IN A VACUUM OF 5×10^{-6} TORR. RHEADS RESULTS IN NITROGEN PLUS 5% HYDROGEN AND IN VACUUM ARE ALSO SHOWN

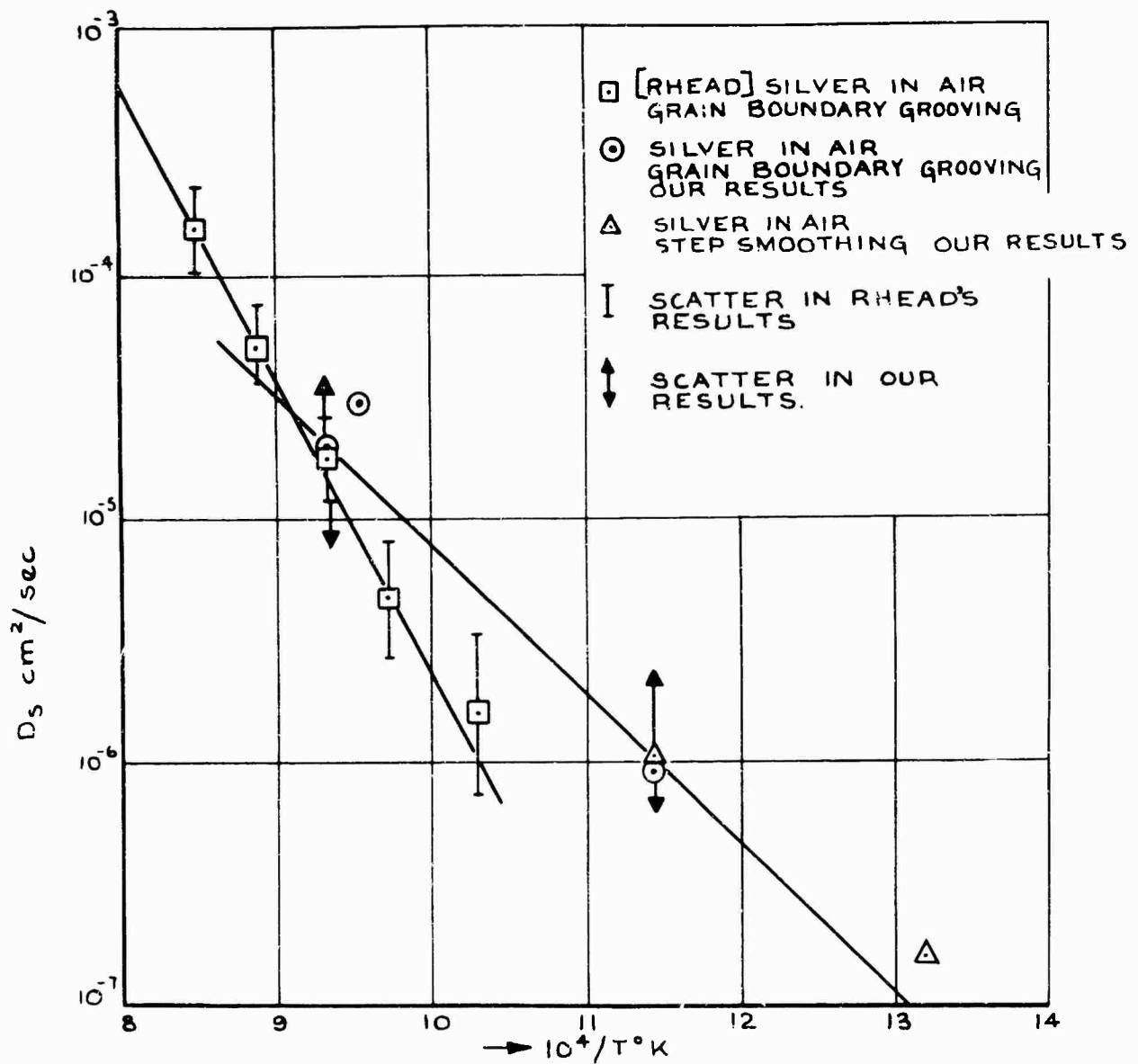


FIG. 11. SURFACE SELF-DIFFUSION COEFFICIENT FOR SILVER HEATED IN AIR

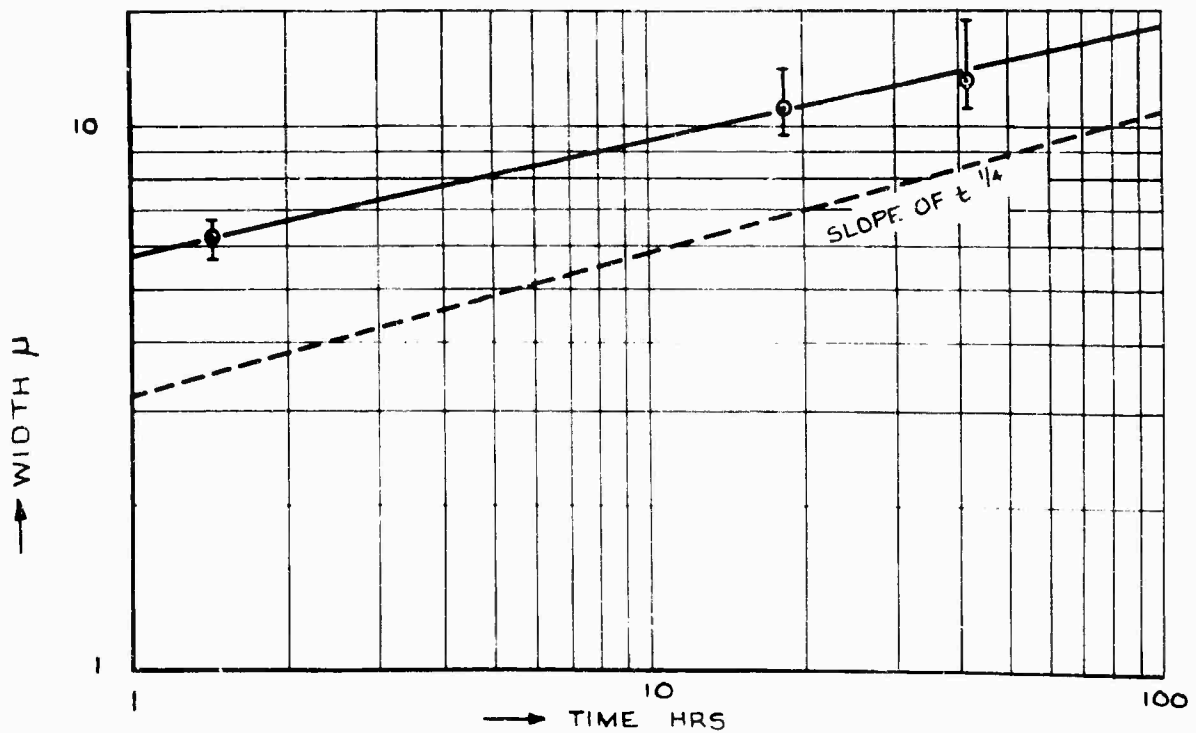
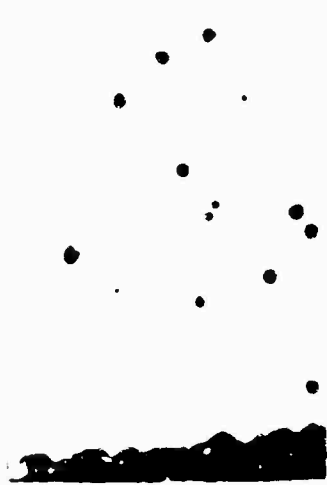


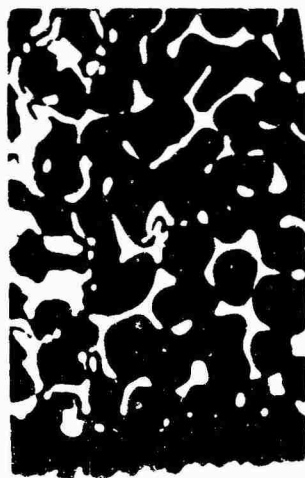
FIG. 12. GROWTH OF THE WIDTHS OF GRAIN BOUNDARIES WITH TIME FOR SILVER HEATED IN AIR AT 800°C



Time: 1½ mins.



Time: 3½ mins.



Time: 8 mins.



Time: 65 mins.

Scale:

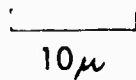


Fig.13. An example of the growth sequence when a film of silver on mica is heated in air at 360°C. Thickness of film $\sim 1100\text{Å}$

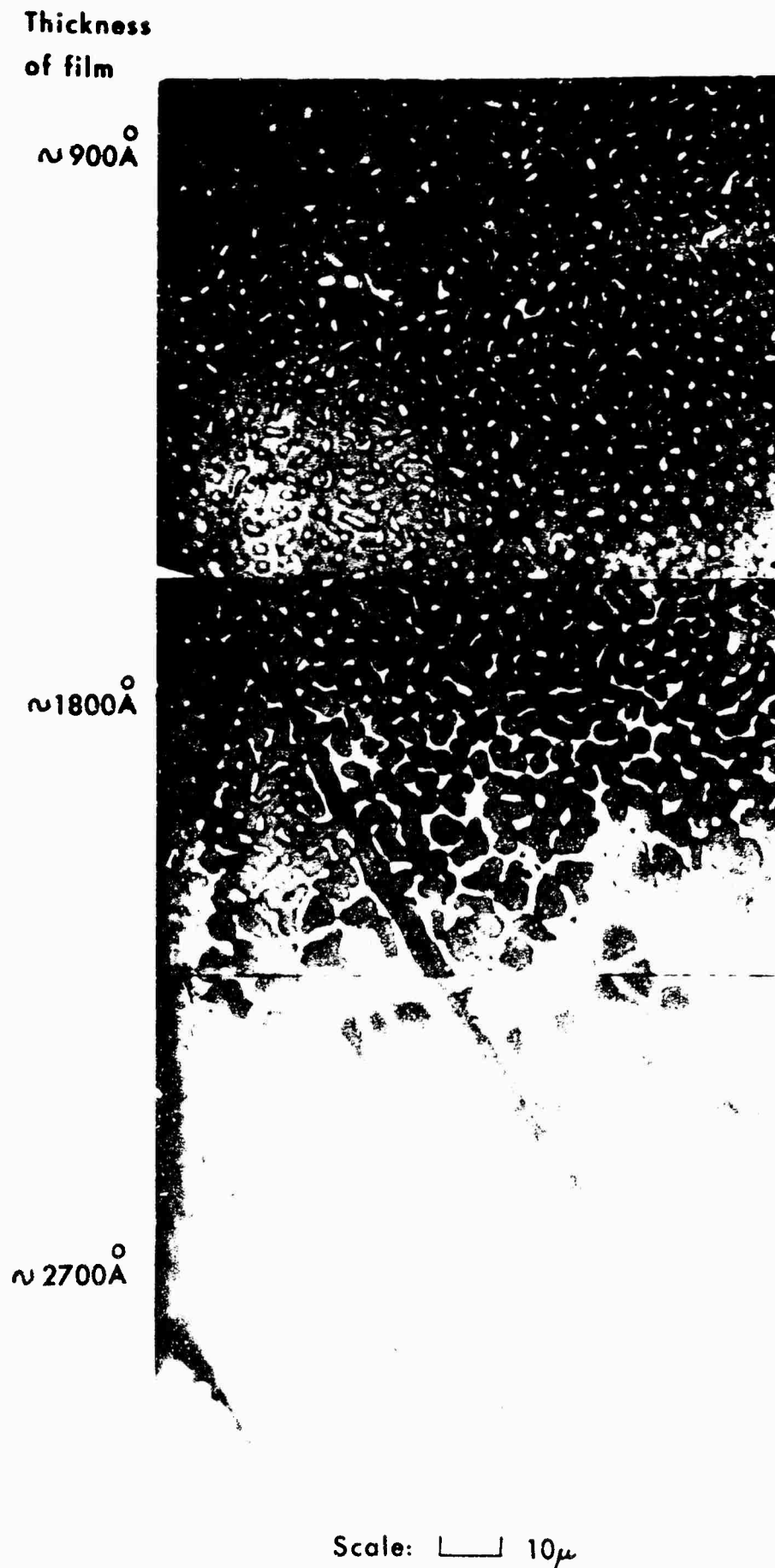


Fig. 14. A wedge shaped film of silver on mica after it has been heated at 300°C for 2 hours in air

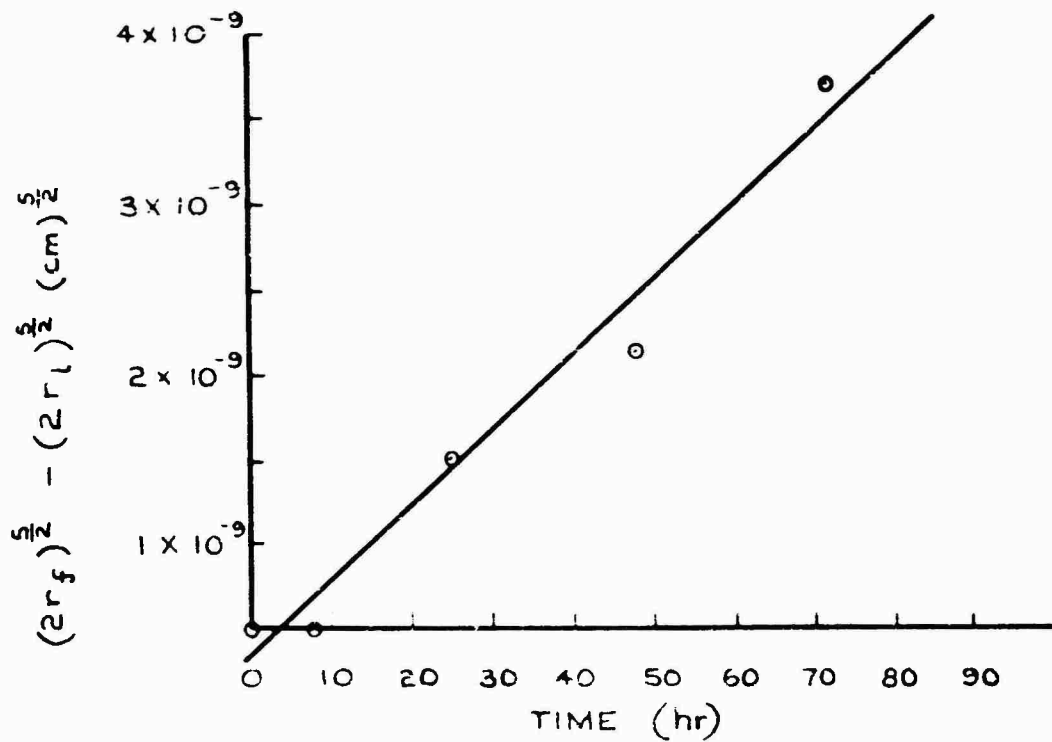


FIG. 15. (a)

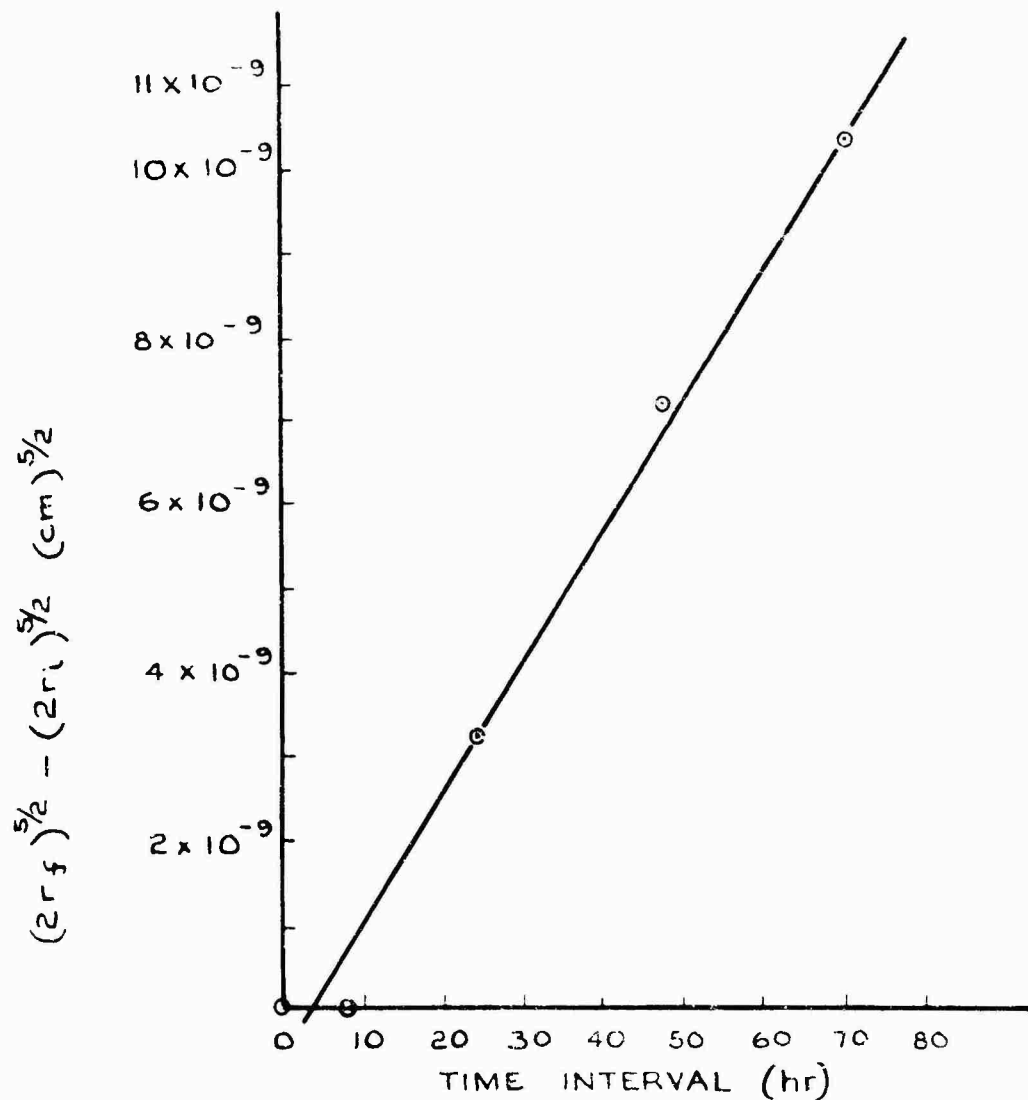


FIG. 15. (b)

FIG. 15. GRAPHS OF $(\text{FINAL DIAMETER OF HOLE})^{5/2} - (\text{INITIAL DIAMETER OF HOLE})^{5/2}$ AGAINST TIME INTERVAL FOR A HOLE IN A SILVER FILM OF THICKNESS 1.1×10^{-5} cm ON MICA WHEN HEATED IN AIR AT 175°C

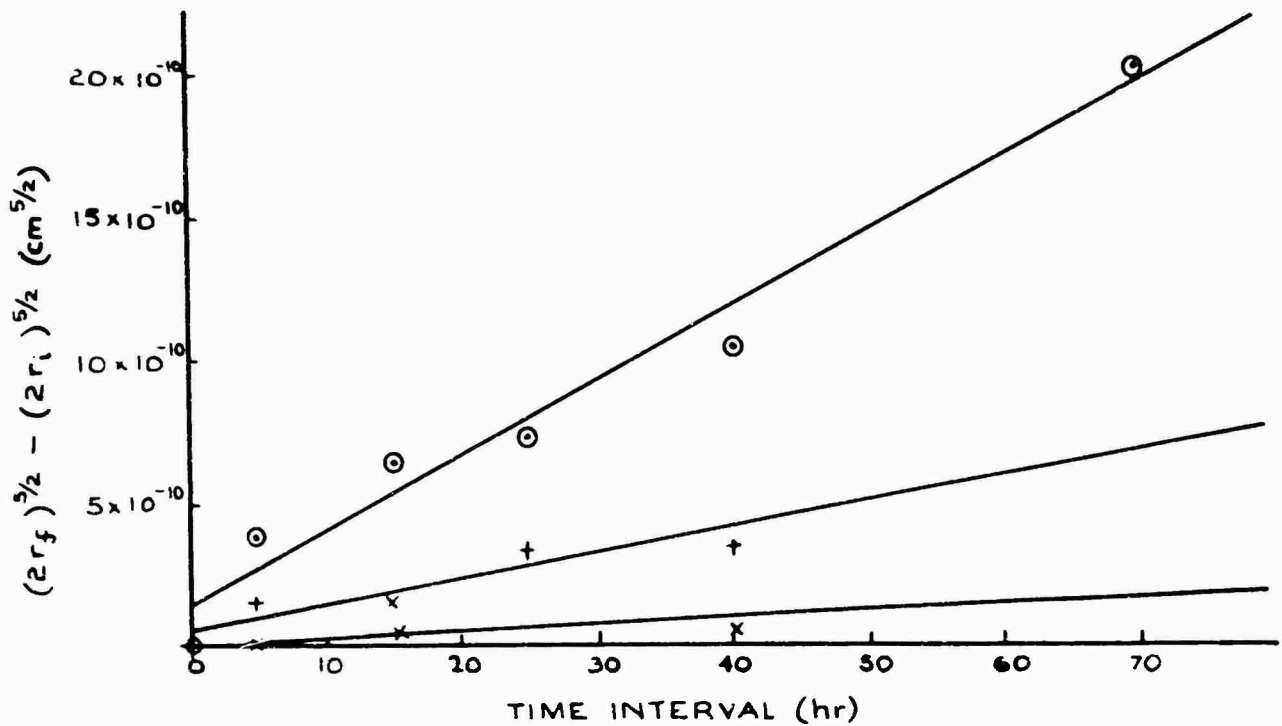


FIG. 16 (a)

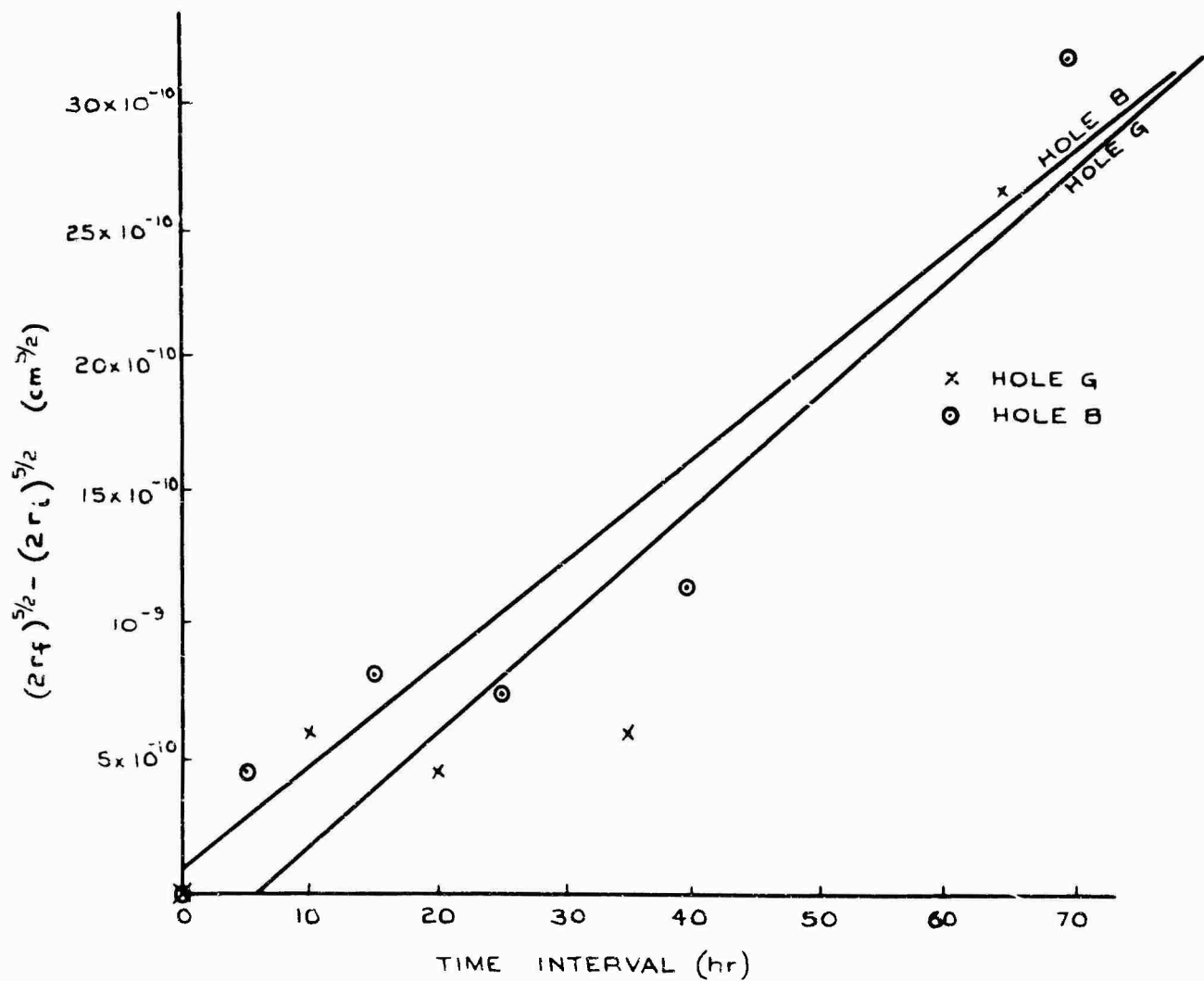


FIG. 16. (b)

FIG. 16. GRAPHS OF $(2r_f)^{5/2} - (2r_i)^{5/2}$ AGAINST TIME INTERVAL FOR HOLES IN A SILVER FILM OF THICKNESS 1.1×10^5 cm ON MICA WHEN HEATED IN AIR AT 265°C

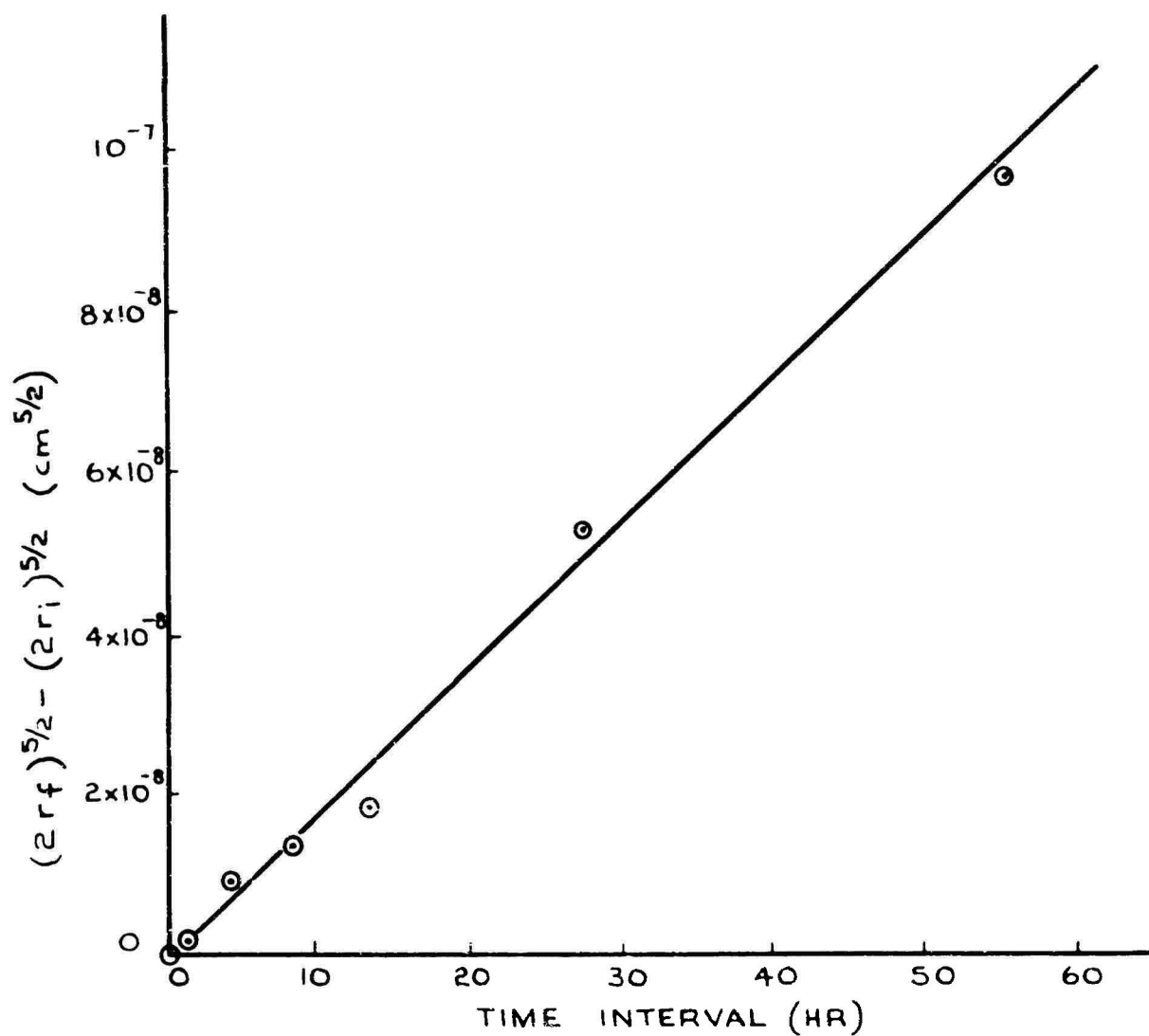


FIG. 17. GRAPH OF $(2r_f)^{5/2} - (2r_i)^{5/2}$ AGAINST TIME INTERVAL FOR A HOLE IN A SILVER FILM OF THICKNESS $1.9 \times 10^{-4} \text{cm}$ ON MICA WHEN HEATED IN AIR AT 300°C

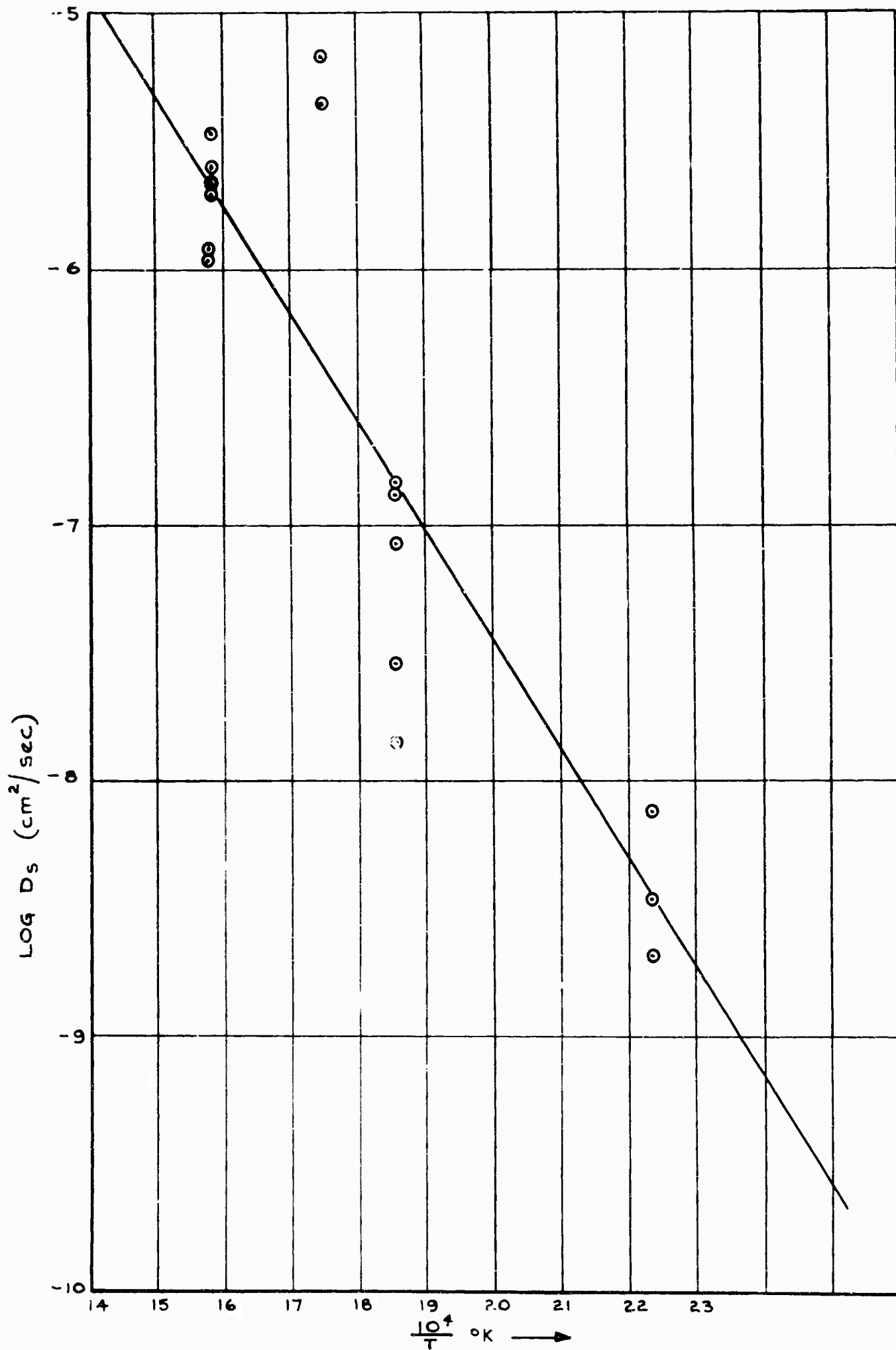
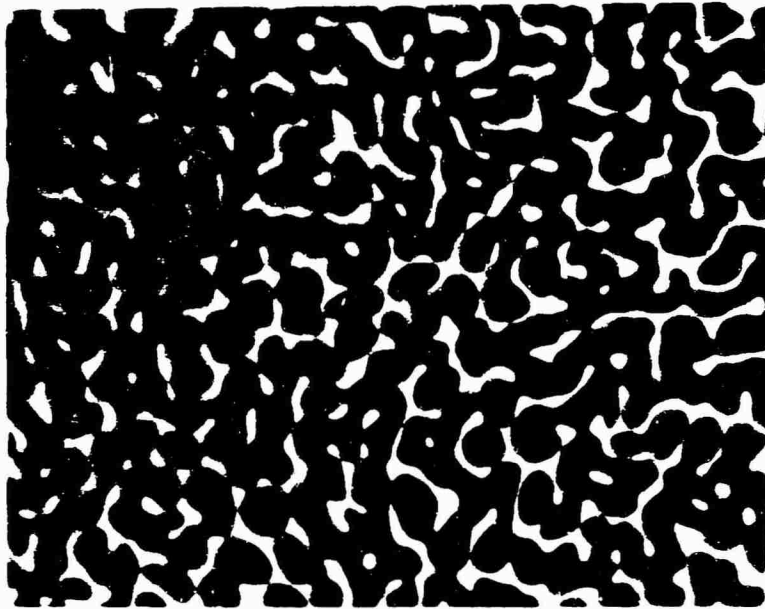
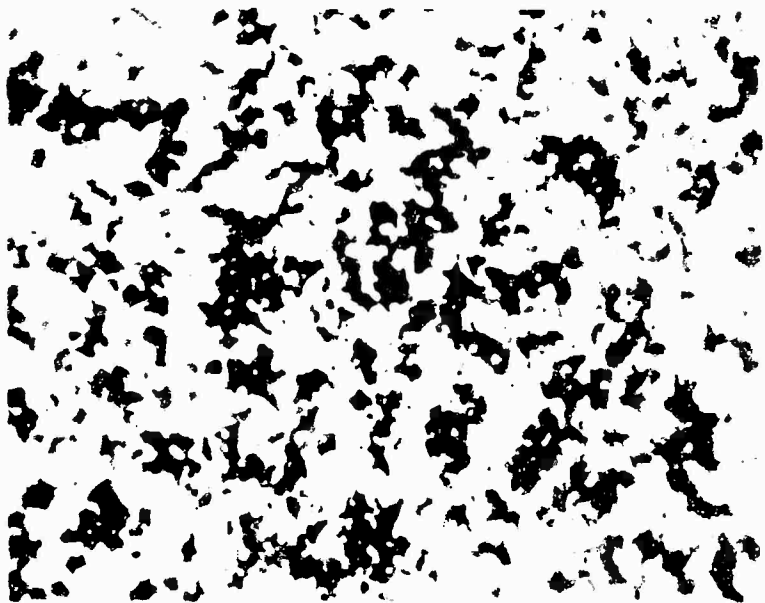


FIG. 18. GRAPH OF LOG D_s AGAINST $10^4/T$ FOR SILVER ON MICA HEATED IN AIR



a. Silver on mica



b. Silver on glass

Scale:  10 μ

Fig.19a&b. Silver films of thickness $\sim 1000\text{\AA}$ on mica and glass substrates after heating for $\frac{1}{4}$ hour at 300°C in air

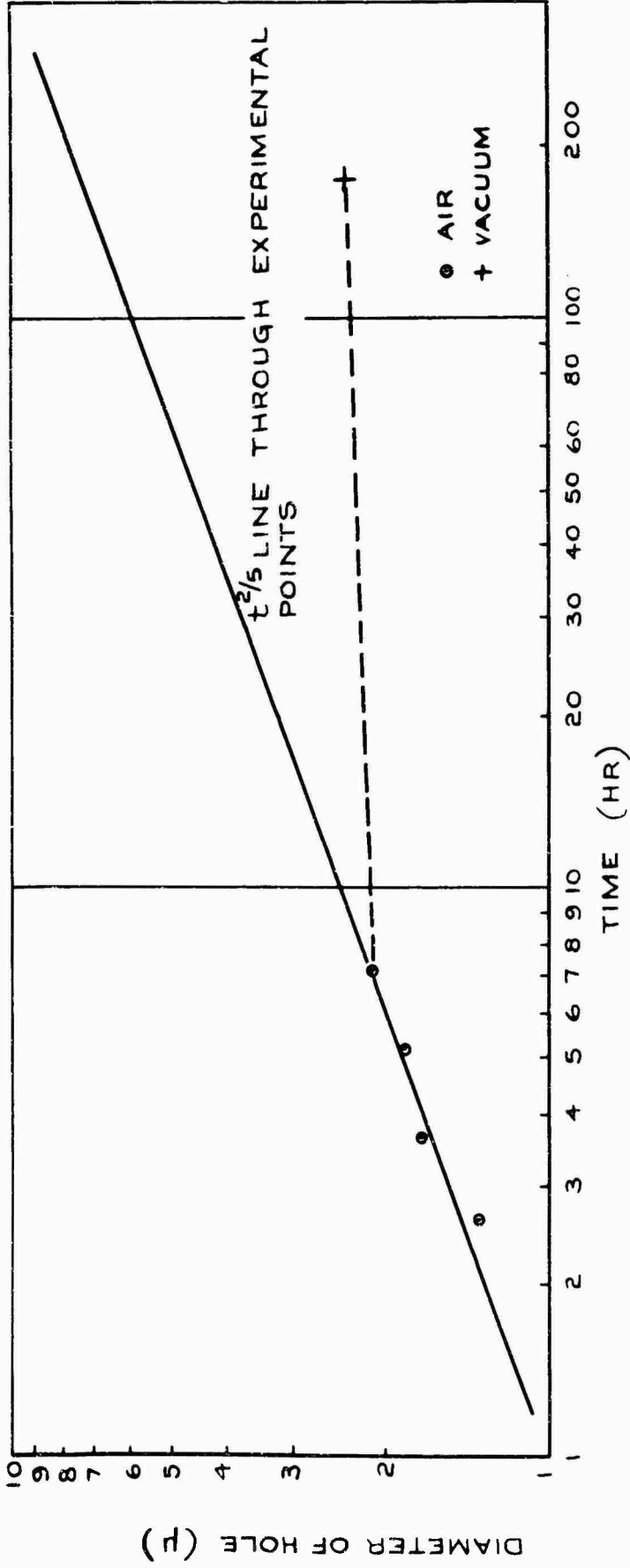


FIG. 20. GRAPH OF THE DIAMETER OF A HOLE AGAINST ESTIMATED TIME SINCE FORMATION OF HOLE FOR SILVER ON MICA AT 265°C